THE JOURNAL OF PHYSICAL CHEMISTRY B

ARTICLE

pubs.acs.org/JPCB

Molecular Dynamics Simulations of the Supramolecular Assembly between an Azobenzene-Containing Surfactant and α-Cyclodextrin: Role of Photoisomerization

Xiaoyan Zheng, Dong Wang,* Zhigang Shuai, and Xi Zhang

MOE Key Laboratory of Organic Optoelectronics and Molecular Engineering, Department of Chemistry, Tsinghua University, 100084 Beijing, People's Republic of China

ABSTRACT: Control of the self-assembly and disassembly at the molecular level has become a subject of increasing activity. The supramolecular assembly between a photoswitchable azobenzene-containing surfactant, AzoC10, and α-cyclodextrin that combines photochemistry and host−guest chemistry for a stimulus-responsive vesicle has been recently reported. To clarify the role of photoisomerization in the reversible assembly and disassembly, we present in this work atomistic molecular dynamics simulations of the host−guest complexation of AzoC10 with α-cyclodextrin. The results of simulation reveal that both *cis*- and *trans*-AzoC10 form the inclusion complexes with α-CD, but the binding modes are rather different. The azobenzene moiety of *trans*-AzoC10 is included at the center of the cavity of α-CD, whereas one of the phenyl rings of *cis*-AzoC10 is exposed to water and the other is included in the cavity of α-CD. The shuttling motion of α-CD over the long alkyl chain of *cis*-AzoC10 is observed in the simulations. The potentials of mean force calculated for AzoC10 to pass through the cavity of α-CD show that the host−guest assembly is basically downhill for *trans*-AzoC10, but an energy barrier has to be overcome for *cis*-AzoC10 to complex with α-CD.

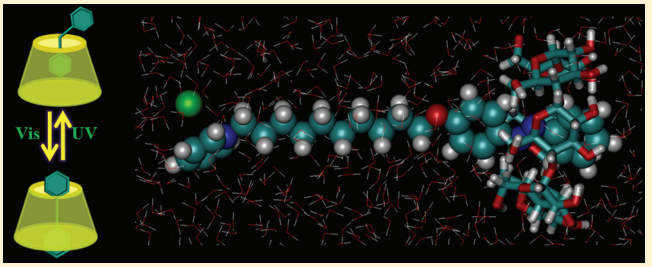

1. INTRODUCTION

The supramolecular assembly generates from its components a well-defined supramolecular architecture that undergoes extended self-assembly. Supramolecular assembly and disassembly based on intermolecular interactions have become an active field during recent decades. In biological processes, molecular assembly is ubiquitous, such as for phospholipids that self-organize into membrane bilayers. Today, synthetic amphiphilic molecules that aggregate into micelles and vesicles are used as capsules for drug delivery[1] and microreactors for nanoparticle preparation.[2] With new building blocks synthesized, control of self-assembly at the molecular level has become a subject of increasing activity.[3−6]

Host−guest interactions are one of the major types of interactions involved in supramolecular assembly. Indeed, practical applications of host−guest chemistry are very popular in basic laboratory research and in the pharmaceutical and food industries. α-Cyclodextrin (α-CD) is a cyclic oligosaccharide consisting of six α-1,4-D-glucopyranoside units that results from the enzymatic degradation of starch. It has been extensively used as the host molecule in host−guest complexation, as well as in molecular recognition. The most striking feature of α-CD is its ability to admit a variety of appropriately sized guest molecules into the cavity with the formation of inclusion complexes. The recognized potential of α-CD−guest interactions as a model system for enzyme active sites has attracted the attention of many investigators.[7,8] Moreover, the photophysical and photochemical properties of organic molecules included in the cyclodextrin cavity are greatly different from those of the molecules in the bulk solution. Fluorescence intensity enhancement,[9−11] intra-[12−14] and intermolecular[15,16] excimer formation, intramolecular exciplex emission,[17] and room-temperature phosphorescence emission[18−20] have been reported to occur in solution in the presence of CDs.

For a given host−guest system, a fundamental aspect to be understood is the precise manner in which the guest molecule binds to its host. The solid-state complex structure may be obtained through X-ray diffraction, and the solution structure can be studied using NMR and other experimental techniques. However, accurate descriptions of the binding process and binding mode of a guest to its host through computation is needed for the study of the mechanism of binding and especially for the design of new host−guest systems with desired properties. The molecular dynamics (MD) simulation is a promising approach for the prediction of the binding mode of a host−guest system in solution with all-atom models for the guest, the host, and the solvent molecules. During the past several years, many MD simulations of cyclodextrins and their inclusion complexes have been reported.[21−26] MD simulations not only reveal the structural features of inclusion complexes but also provide

Received: August 1, 2011
Revised: December 1, 2011
Published: December 02, 2011

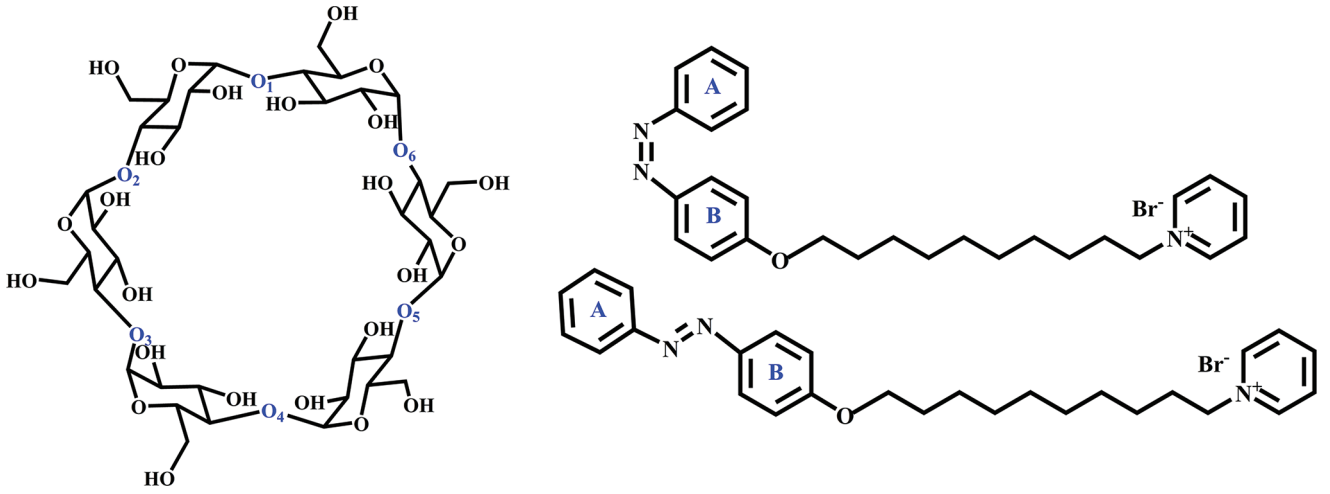

Figure 1. Molecular diagrams of α-CD and AzoC10. The glycosidic oxygen atoms of α-CD and the phenyl rings of AzoC10 are labeled.

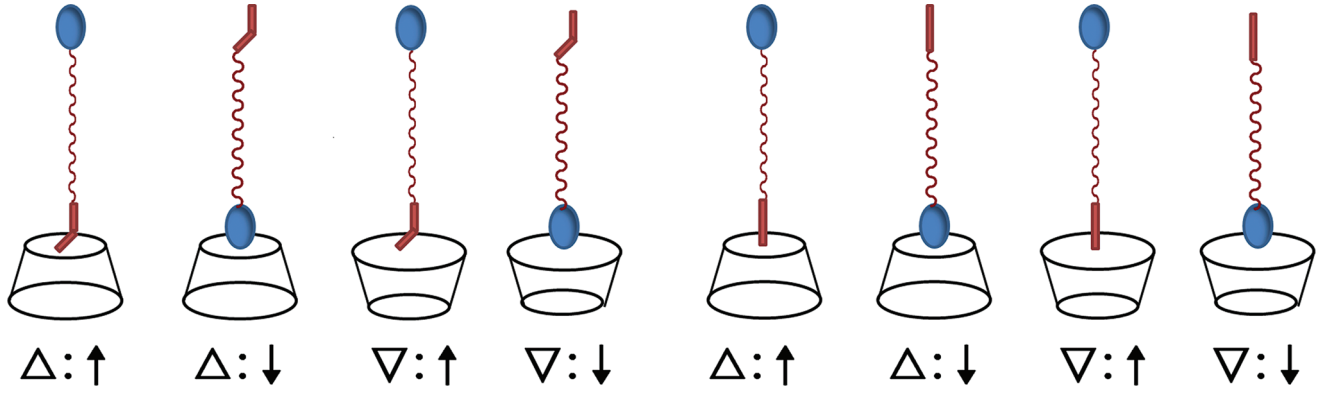

Figure 2. Schematic representation and notations for the starting configurations of the MD simulations. The red bar represents the azobenzene moiety, with the bent one for the cis isomer and the straight one for the trans isomer. The blue ellipse represents the pyridinium headgroup, and the red string represents the long alkyl chain of AzoC10.

insights into the host−guest interactions from dynamic and energetic perspectives.

A model system that combines photochemistry and host−guest chemistry for a stimulus-responsive vesicle has been recently reported.[3] In that study, a surfactant modified by the functional group responsive to light has been fabricated, and the photocontrolled reversible assembly and disassembly between the surfactant and α-CD have been observed. The surfactant designed is 1-[10-(4-phenylazophenoxy)decyl]pyridinium bromide and termed as AzoC10. It is known that the azobenzene moiety can be photoswitched selectively from trans to cis form by UV light, and reversely from cis to trans form by visible light.[27] The *trans*-azobenzene is well-recognized by α-CD; however, when it is transformed to the cis form by photoisomerization, the bulky *cis*-azobenzene cannot be included by α-CD anymore because of the mismatch between the host and guest molecules. The pure AzoC10 is amphiphilic and forms vesicle-like aggregates in aqueous solution. When α-CD is added, the vesicle-like aggregates disassemble. After UV irradiation, vesicle-like aggregates form again, disappearing upon exposure to visible light. As a result, the host−guest assembly and disassembly between azobenzene and α-CD controlled by external photostimuli can act as a driving force to build up molecular shuttles, motors, and machines.[28−34]

To disclose the role of photoisomerization in the reversible assembly and disassembly, we study the inclusion of AzoC10 with α-CD by use of the MD simulations. To this end, the inclusion dynamics, the binding mode of the guest to its host, the structural changes induced by the host−guest interactions, the role of hydrogen bonds and water molecules in the supramolecular assembly, and the potentials of mean force for the guest to pass through the cavity of the host have been thoroughly analyzed for both cis and trans conformers of the guest molecule. The investigations at the molecular level are expected to be helpful in the design of new building blocks for control of the supramolecular assembly and disassembly in aqueous solution.

2. MODEL AND SIMULATION METHOD

Model Setup. Figure 1 shows the molecular diagrams of α-CD and *cis*- and *trans*-AzoC10. α-CD is a cyclic oligosaccharide consisting of six α-1,4-glucopyranoside units. The primary and secondary hydroxyl groups of α-CD are respectively located at the narrow and wide rims of the torus. The primary hydroxyl groups are directed toward the exterior of α-CD, so the primary

dx.doi.org/10.1021/jp2073107 |*J. Phys. Chem. B* 2012, 116, 823–832

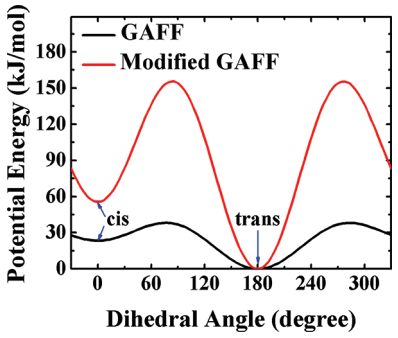

Figure 3. Reparametrization of the GAFF. The potential energy curves along the dihedral angle C−N═N−C coordinate were displayed for both the original GAFF and the modified one. The dihedral angle of 0° and 180° corresponds to the cis and trans conformers, respectively. The force field parameters were modified to reproduce the DFT-calculated energy barrier for the cis−trans conversion, as well as the energy difference between the cis and trans conformers. The detailed procedure of parametrization can be found in the main text.

rim of α-CD is somehow hydrophobic. The interior of the cavity is composed of a circle of C−H groups, a circle of glycosidic oxygens, and another circle of C−H groups; therefore, the interior of α-CD is hydrophobic. The nonbonding electron pairs on the α-1,4-glucopyranoside oxygen bridges are directed toward the interior of the cavity, producing a high electron density there and conveying some Lewis base characteristics. The structural features of native α-CD allow it to host hydrophobic species in its cavity, giving rise to inclusion complexes.[35−37] The guest molecule AzoC10 is amphiphilic. The hydrophilic head of AzoC10 is a pyridinium group with a positive charge on the nitrogen atom. The alkyl chain and the azobenzene moiety are hydrophobic.

It is usually unlikely to see the spontaneous formation of all the inclusion complexes in typical simulation times, so we start the simulations from all possible orientations of AzoC10 relative to α-CD. To identify these configurations, the following notations are used in the paper: Δ and ▽ represent α-CD with its primary rim up and down, and ↑ and ↓ stand for AzoC10 with its hydrophilic head up and down, respectively. Thus, the initial configurations Δ:↑, Δ:↓, ▽:↑, and ▽:↓ represent all possible orientations that α-CD and AzoC10 adopt in the inclusion complexes as illustrated in Figure 2.

Simulation Details. Molecular dynamics simulations were carried out using the GROMACS software package (version 3.3.3).[38,39] GLYCAM06 force field[40,41] parameters were used for α-CD. The atom types and parameters of AzoC10 were built from the general amber force field (GAFF).[42] The electrostatic potential of AzoC10 was calculated by the HF/6-31G* method using the Gaussian09 package,[43] and the partial charges of the atoms reproducing the electrostatic potential were obtained by using the restrained electrostatic potential (RESP) fit method.[44,45] The targeted host and guest molecules were placed in a cubic box of pre-equilibrated TIP3P water molecules.[46] The box length was 6 nm, containing one host, one guest, and 7000 water molecules. The size of the simulation box was so large that interactions between a molecule and its periodic images were avoided to correctly simulate an infinitely diluted solution. To neutralize the charge of the ionic head of the surfactant, one bromide ion per AzoC10 molecule was added. All simulations were performed with the *NPT* ensemble at $T = 300$ K and $P = 1$ atm. Newton's classical equations of motion were integrated at a time step of 1 fs using the classical leapfrog algorithm. Weak couplings to external heat and pressure baths were applied based on the Berendsen scheme.[47] Before starting MD simulations, energy minimization using the steepest descent algorithm was performed. Periodic boundary conditions were applied in all three directions to minimize the edge effects in a finite system. The reciprocal space sum of the electrostatic interactions was evaluated by the particle mesh Ewald (PME) method,[48,49] and the direct space sum was calculated at a cutoff distance of 1.0 nm. Each system was simulated for 10 ns, with configurations stored every 1 ps for analysis. To better simulate the host−guest interactions, no constraints to the solute and solvent molecules were applied. Trajectory analysis was performed by use of the utilities in the GROMACS package[38] and the VMD package.[50]

The potentials of mean force (PMF) for both *cis*- and *trans*-AzoC10 to pass through the cavity of α-CD were calculated with the umbrella sampling method.[51] The center-of-mass distance between α-CD and the azobenzene moiety of the guest molecules was used to define the reaction coordinate. In the simulation box, α-CD was oriented such that the normal of its six glycosidic oxygen plane was in the direction of z axis, and a harmonic positional restraint was imposed on the six oxygen atoms with a force constant of 1000 kJ/mol/nm^2 in the x, y, and z directions, respectively. During the umbrella sampling simulations, a harmonic biasing potential with a force constant of 2000 kJ/mol/nm^2 was imposed on the center-of-mass distance between α-CD and the azobenzene moiety of the guest molecule. For AzoC10 to translocate from one side of α-CD to the other, the reference coordinate varies from −3 to 2 nm with an increment of 0.05 nm, amounting to a total of 100 windows for each PMF. For each window, the simulation consists of 200 ps of equilibration followed by 300 ps of production run, so the total simulation time for each PMF was 50 ns. The potentials of mean force were constructed by using the weighted histogram analysis method (WHAM).[51−54]

Force Field Modification. The force field parameters for AzoC10 were adopted from the GAFF[42] that was developed for organic and pharmaceutical molecules composed of H, C, N, O, S, P, and halogens. During the simulations, we found that *cis*-AzoC10 can easily transform into *trans*-AzoC10 when interacting with α-CD. After careful inspection, we confirmed that this conformational change was caused by the inappropriate force field parameters of the dihedral angle C−N═N−C term. In fact, in the ground state, the potential energy barrier for the cis to trans conversion is over 100 kJ/mol based on earlier ab initio calculations.[55,56] However, the soft torsional angle parameters of the GAFF pose a potential energy barrier of only about 26 kJ/mol, which can be easily overcome when host−guest interactions exist. In the simulations, we found that *trans*-AzoC10 fits into the cavity of α-CD very well so it forms a stable inclusion complex with α-CD in aqueous solution. On the other hand, the cavity of α-CD cannot include the bulky head of *cis*-AzoC10, but cis to trans conversion occurs from the strong hydrophobic interactions between the host and guest molecules. To correctly describe the interactions between α-CD and AzoC10, we modified the force field parameters of the C−N═N−C dihedral angle term, which is the main potential energy term responsible for the isomerization of the azobenzene moiety. In the GAFF, the potential energy profile of the dihedral angle C−N═N−C takes the functional form $E = V_1(1 + \cos\phi) + V_2[1 + \cos(2\phi - 180)]$. In the modification, the functional form of the energy profile was not changed, but the two parameters V_1 and V_2 were adjusted.

dx.doi.org/10.1021/jp2073107 |*J. Phys. Chem. B* 2012, 116, 823–832

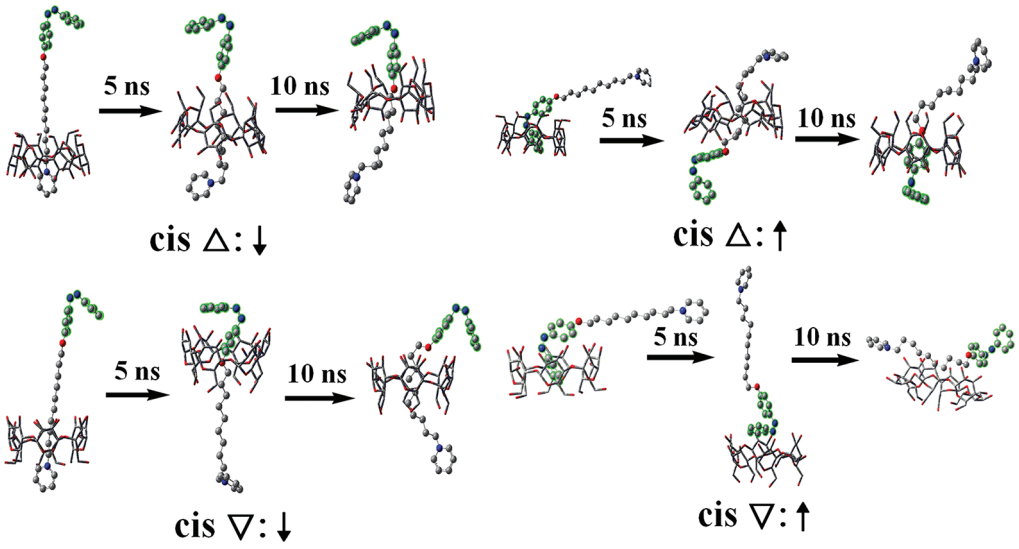

Figure 4. Snapshots of the crucial phases in the process of assembly between α-CD and *cis*-AzoC10. The solvent molecules are not shown for clarity. α-CD is represented by sticks, and *cis*-AzoC10 is represented by sphere and sticks with the azobenzene moiety highlighted in green.

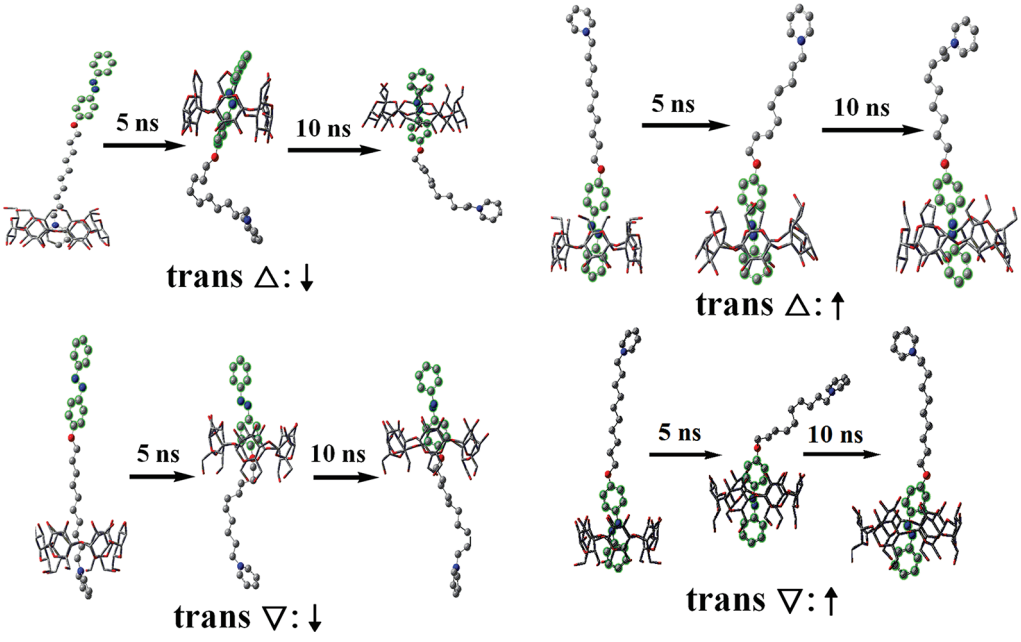

Figure 5. Snapshots of the crucial phases in the process of assembly between α-CD and *trans*-AzoC10. The solvent molecules are not displayed for clarity. α-CD is represented by sticks, and *trans*-AzoC10 is represented by sphere and sticks with the azobenzene moiety highlighted in green.

To determine V_1 and V_2, we need the energy barrier for the cis to trans conversion, as well as the energy difference between the cis and trans conformations. The energy barrier we used is 100 kJ/mol, taken from ref 56, in which a scan of the energy surface along the torsion angle was performed on the azobenzene molecule at a step size of 20° using the density functional theory (DFT) in the local-density approximation. Their DFT calculated barrier is in quite reasonable agreement with the experimental estimates of the activation energy for a series of azobenzene compounds in solution.[57] The energy difference between the cis and trans conformation is obtained from our calculations on the AzoC10 molecule at the B3LYP/6-31G(d) level of theory using the Gaussian09 package.[43] The modified potential energy curve was shown in Figure 3 in comparison with the original one. After modification, the cis−trans conversion of the azobenzene moiety was no longer observed during the simulations.

3. RESULTS AND DISCUSSION

As described earlier, we built the initial configurations of simulations based on four different arrangements of the α-CD and AzoC10 host−guest system. The host−guest system was then placed in a cubic box of water that was pre-equilibrated at $T = 300$ K and $P = 1$ atm. For each initial configuration, several simulations with random velocity distributions have been performed, each of duration 10 ns. In each simulation, the root-mean-square

dx.doi.org/10.1021/jp2073107 |*J. Phys. Chem. B* 2012, 116, 823–832

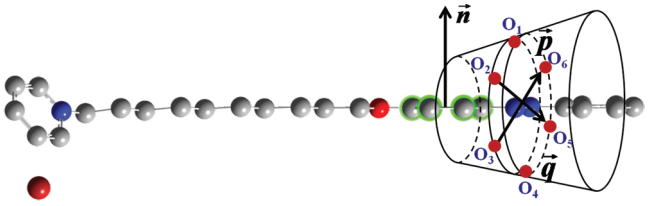

Figure 6. Definitions of three vectors used to describe the induced structural changes of both the host and guest molecules. $\vec{p}$ and $\vec{q}$, respectively, represent vectors connecting two facing glycosidic oxygen atoms. $\vec{n}$ is the normal vector of one of the phenyl ring planes of AzoC10. Note that $\vec{p}$, $\vec{q}$, and $\vec{n}$ are not necessarily coplanar.

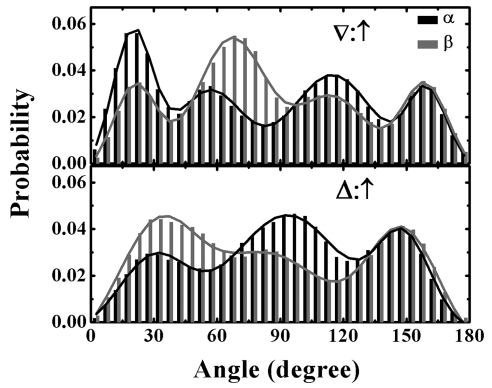

Figure 7. Probability distributions of the angles α and β defined in Figure 6, estimated after the α-CD/*trans*-AzoC10 complex has formed in the aqueous solution. The results obtained from the simulations with the initial configurations ∇:↑ and Δ:↑ that represent two possible arrangements of *trans*-AzoC10 within α-CD, are respectively displayed in the upper and lower panels.

deviations (RMSDs) of the host−guest structure to the initial structure were calculated. It is found that after 2 ns, the host−guest system is usually equilibrated with an average rmsd of 0.1 nm. The amplitude of fluctuations of the RMSDs is about 0.02 nm after equilibration. In the following probability distribution analysis, the initial 2 ns of trajectories is the equilibration stage, and the remaining 8 ns is used for data production.

Formation of the Inclusion Complexes in Aqueous Solution. As can be seen from Figure 4, for the α-CD and *cis*-AzoC10 assembly starting from the Δ:↓ and ∇:↓ configurations, we have placed the polar head of *cis*-AzoC10 into the hydrophobic cavity in the initial configurations. Because the positively charged head is hydrophilic, it went through the cavity and pulled the hydrophobic alkyl chain into the cavity until the azobenzene moiety was close to the rim of α-CD. For the α-CD and *cis*-AzoC10 assembly starting from the Δ:↑ and ∇:↑ configurations, we put one phenyl ring of the azobenzene moiety into the hydrophobic cavity of α-CD in the initial configuration. In the 10 ns simulation, we found that for the assembly starting from the Δ:↑ arrangement, the azobenzene moiety squeezed through the primary rim and into the cavity of α-CD. Because the *cis*-azobenzene moiety is strongly nonplanar, it does not match the cavity size of α-CD. As a result, the *cis*-azobenzene moiety went through the cavity and was exposed to the bulk at the secondary rim. The long hydrophobic alkyl chain was encapsulated inside the cavity. Moreover, we observed that the long alkyl chain shuttled back and forth in the hydrophobic cavity, and it did not bind specifically to the cavity wall.

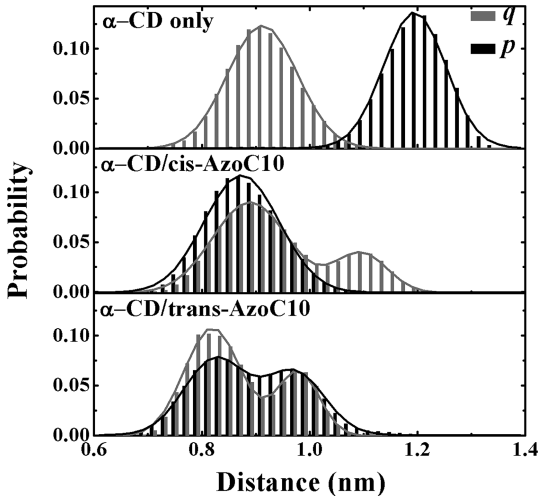

Figure 8. Probability distribution of the distances between two facing glycosidic oxygen atoms that are used to define the vectors $\vec{p}$ and $\vec{q}$. The results shown in the upper panel are from the simulation of pure α-CD, and those in the lower two panels are from the simulations of the host−guest system.

As for the simulations starting from the ∇:↑ configuration, we did not see the azobenzene moiety squeeze through the wide rim of α-CD. In a typical simulation, the benzene ring initially placed inside the cavity went out of the cavity and formed the $\pi-\pi$ stacking with the secondary hydroxyl oxygen atoms of α-CD. At the end of the 10 ns simulation, *cis*-AzoC10 was found to lie down on top of the secondary rim of α-CD, perpendicular to the central axis of α-CD. There are several reasons for *cis*-AzoC10 not entering the cavity of α-CD in this case: (1) the steric hindrance of the *cis*-azobenzene moiety; (2) the hydrophilicity of the secondary rim; (3) the stable intra- and intermolecular hydrogen bond networks at the secondary rim of α-CD. As can be seen, the secondary rim is relatively rigid, and it is difficult for the bulky hydrophobic *cis*-azobenzene to enter the cavity from the side of secondary rim.

As for the α-CD and *trans*-AzoC10 assembly shown in Figure 5, the simulation results suggest regardless of the initial configurations, the structures of the inclusion complexes formed between α-CD and *trans*-AzoC10 are similar. Because of the dipole−dipole interactions[58−60] between azobenzene and α-CD, the azobenzene moiety is included axially in the cavity of α-CD.

Structural Changes Induced by the Host−Guest Interactions. The host−guest interactions between α-CD and AzoC10 have caused the structural changes of the host and guest molecules. To depict the induced structural changes of α-CD, three vectors $(\vec{p}, \vec{q}, \vec{n})$ have been defined as illustrated in Figure 6. The vector $\vec{p}$ connects two facing glycosidic oxygen atoms, O_3 and O_6, and the vector $\vec{q}$ connects O_2 and O_5 in the central section of the cavity. $\vec{n}$ is the normal vector of the B phenyl ring plane of azobenzene in *trans*-AzoC10. Note that the three vectors $\vec{p}$, $\vec{q}$, and $\vec{n}$ are not necessarily coplanar. The angle α is defined as the angle between $\vec{p}$ and $\vec{n}$, and β is the angle between $\vec{q}$ and $\vec{n}$. The angle $\alpha = 0°$ corresponds to the vector $\vec{p}$ being parallel to $\vec{n}$. The angles α and β are used to describe the orientation of *trans*-AzoC10 within the cavity of α-CD. To analyze the degrees of freedom of *trans*-AzoC10 inside α-CD, the probability distributions of α and β were calculated after the inclusion complex has

dx.doi.org/10.1021/jp2073107 |*J. Phys. Chem. B* 2012, 116, 823–832

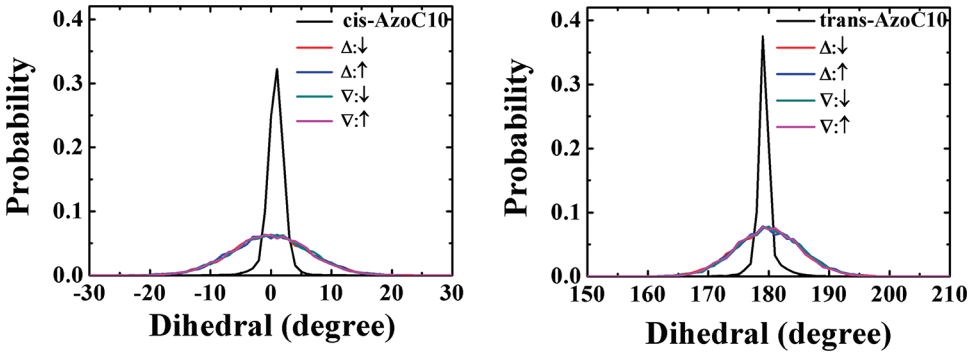

Figure 9. Probability distribution of the dihedral angle (C−N═N−C) of AzoC10 in the presence and absence of the host molecule for all possible arrangements of the initial configurations (cis: left; trans: right).

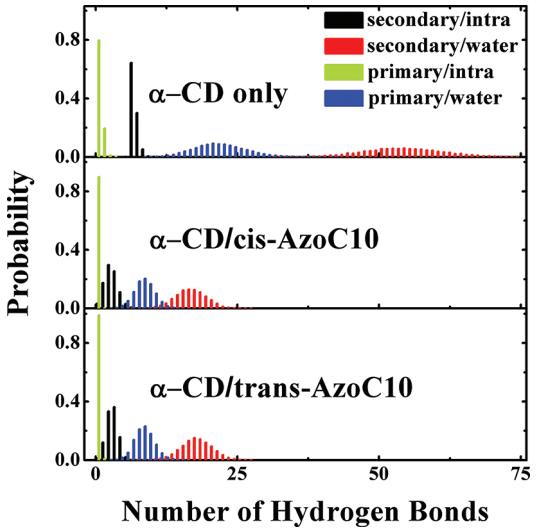

Figure 10. Probability distribution of the number of intramolecular hydrogen bonds formed within the primary and secondary rims of α-CD and that of intermolecular hydrogen bonds formed between the rims of α-CD and water, for α-CD only (upper), α-CD/*cis*-AzoC10 (middle), and α-CD/*trans*-AzoC10 (lower), respectively, in aqueous solution. The trajectories starting from the initial configuration Δ:↑ were used for analysis. The legends secondary/intra, secondary/water, primary/primary, and primary/water, respectively, represent the hydrogen bonds formed within the hydroxyl groups of the secondary rim of α-CD, between the hydroxyl groups of the secondary rim and water, within the hydroxyl groups of the primary rim of α-CD, and between the hydroxyl groups of the primary rim and water.

formed, and the result was shown in Figure 7. The probability distribution of each angle is defined as the frequency of occurrence of a particular value of that angle. For the α-CD/*trans*-AzoC10 inclusion complex, the translational motion of *trans*-AzoC10 in the cavity of α-CD is small. The standard deviation of the center-of-mass displacement between α-CD and the azobenzene moiety is 0.05 nm. The distributions of α and β reflect mainly the rotations of the guest molecule.

As can be seen from Figure 7, for the α-CD/*trans*-AzoC10 complex, both α and β do not fluctuate around an equilibrium value, instead, there exist several preferential orientations for the azobenzene moiety. The probability distributions of α and β for the simulations starting from different initial configurations are quite similar: both angles exhibit a broad distribution, suggesting that the phenyl ring of *trans*-AzoC10 rotates inside the cavity of α-CD. Along the rotation path, there exist two energy barriers located at 0° and 180° for both α and β. Because the nonplanar azobenzene moiety of *cis*-AzoC10 did not enter the cavity of α-CD, we did not monitor the phenyl ring motion of the α-CD/*cis*-AzoC10 complex.

The probability distributions of the distances between two facing glycosidic oxygen atoms of α-CD, which have been used to define the vectors $\vec{p}$ and $\vec{q}$, are calculated. The distributions obtained from the simulations of pure α-CD, α-CD/*cis*-AzoC10, and α-CD/*trans*-AzoC10 in aqueous solution are displayed in Figure 8. It can be seen that with only α-CD in solution, the peak distribution of the length of $\vec{p}$ is different from that of $\vec{q}$, which indicates that the distances between two facing glycosidic oxygen atoms, p and q, are not equal. Therefore, in the absence of the guest molecule, the cavity of α-CD shows poor symmetry with notable elongation in the direction of $\vec{p}$. It is further noted that once such a conformation is achieved, it cannot convert to an equivalent asymmetric one, but it remains stable for the total simulation time. Inspection of the trajectories suggests that this is an effect of stabilization by intermolecular H-bonds with water molecules at the rims of α-CD and hydrophobic collapse of the cavity of α-CD. By contrast, in the simulations of the host−guest system, it is found that interactions between α-CD and AzoC10 have caused structural changes of α-CD. The cavity of α-CD becomes more symmetric with the guest molecule included in it.

To analyze the structural changes of the guest molecule caused by the interactions with the host, the probability distributions of the dihedral angle (C−N═N−C) of *cis*-AzoC10 and *trans*-AzoC10 are obtained from the simulations of pure AzoC10 and α-CD/AzoC10. In the simulations of the host−guest system, trajectories starting from all possible initial configurations are examined and the results are summarized in Figure 9. In the case of pure *cis*-AzoC10 in solution, obviously the distribution of the dihedral angle C−N═N−C exhibits a sharp peak around 0°, which indicates that the guest molecule remains in the cis form during the simulation. After complexation with the host, the dihedral angle fluctuates around 0°, too, but the distributions are much broader, with the full width at half-maximum of about 15°. In addition, the probability distributions do not rely on the initial configurations of the simulations. The same observations apply to *trans*-AzoC10 as well, except that the dihedral angle C−N═N−C of *trans*-AzoC10 fluctuates around 180°, and the distributions are slightly narrower than those of *cis*-AzoC10 for both pure guest molecule and the host−guest system. Overall,

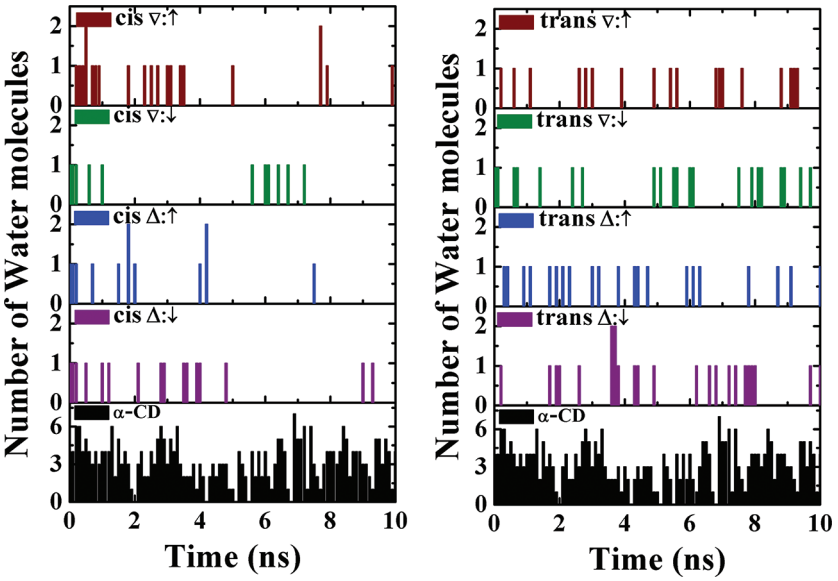

Figure 11. Number of water molecules inside the cavity of α-CD in the presence and absence of the guest molecule, monitored as a function of the simulation time. The trajectories starting from all possible initial configurations have been analyzed for both *cis*-AzoC10 and *trans*-AzoC10.

after complexation, the dihedral angle fluctuates more easily due to the interactions with the host, but AzoC10 remained in either cis or trans conformation throughout the 10 ns simulations. Besides, in comparison with *cis*-AzoC10, the trans structure seems to be more rigid.

Hydrogen Bond Analysis. There are six and twelve hydroxyl groups located at the primary and secondary rims, respectively. Therefore, α-CD forms not only intramolecular hydrogen bonds but also intermolecular hydrogen bonds with the water molecules in solution. In the process of complexation with the guest molecule, these hydrogen bond networks could be broken. To show how hydrogen bonds change before and after the formation of the inclusion complexes, the number of intramolecular hydrogen bonds formed within the hydroxyl groups of the primary and secondary rims of α-CD, and the number of intermolecular H-bonds formed between the rims and the water molecules, were monitored during the 10 ns simulations. We used a donor−acceptor cutoff distance of 0.35 nm and a hydrogen-donor−acceptor angle less than 30° as the criteria for the hydrogen bond formation. The results are collected in Figure 10. It is clear that the number of H-bonds formed in the α-CD/*cis*-AzoC10 and α-CD/*trans*-AzoC10 complexes are similar. Because the primary hydroxyl groups are oriented toward the exterior of α-CD and the distance between adjacent oxygen atoms is too large to form H-bonds, the number of intramolecular H-bonds formed within the primary rim of α-CD remained null throughout the simulation, whether or not the inclusion complex has formed. Other than that, the number of H-bonds has reduced substantially after complexation. The distance between the neighboring hydroxyl oxygens of the secondary hydroxyl groups is close enough to form H-bonds, and the corresponding intramolecular H-bonds within the secondary rim of α-CD reduced to two or three upon complexation. The number of H-bonds between the primary hydroxyl groups and water reduced to seven or eight, and that between the secondary hydroxyl groups and water reduced to fifteen to seventeen. As shown above, the primary and secondary rims are quite different. Compared with the primary rim, the secondary rim has more water molecules around, and they form stable hydrogen bond networks. Thus, it is not easy for the guest molecule to enter the cavity of α-CD from the side of the secondary rim.

Water Molecules inside the Cavity of α-CD. Water molecules play an essential role in the host−guest complexation and the supramolecular assembly in aqueous solution. The number of water molecules inside the cavity of α-CD was monitored during the simulation. To count the number of water molecules inside the cavity, we defined a sphere centered at the geometrical center of the six oxygen atoms bridging the glucopyranoside rings, with a diameter of 0.90 nm. This diameter corresponds to the largest distance between two oxygen atoms linking the glucopyranoside units in the fully optimized structure of α-CD. The definition allows us to monitor the time evolution of the number of water inside the preformed complexes unambiguously and, in turn, makes it possible to guard the solute−solute and solute−solvent interactions in the process of the supramolecular assembly.

In aqueous solution, the nonpolar α-CD cavity is occupied by water molecules, but these polar−nonpolar interactions are energetically unfavored. Therefore, these water molecules can be readily substituted by appropriate "guest molecules", which are less polar than water. The release of water molecules from the α-CD cavity to the bulk water[61] are the "driving force" for the complexes to form. The substitution of these high-enthalpy water molecules by an appropriate "guest molecule" is the major feature of the host−guest interactions.

Without the guest molecule, α-CD often hosts four to six water molecules in its cavity, as indicated by the histogram in Figure 11. In the X-ray crystal structures of α-CD, five to six water molecules were found in the cavity of α-CD, with two of them bonded to the peripheral hydroxyl groups of α-CD,[62] which suggests that our results of simulation are quite reasonable. After complexation with either *cis*-AzoC10 or *trans*-AzoC10, α-CD hosts at most one to two water molecules, and most often the cavity is not occupied by water. It shows that the interior of the cavity is hydrophobic, and water molecules bind loosely to the cavity of α-CD.

dx.doi.org/10.1021/jp2073107 |*J. Phys. Chem. B* 2012, 116, 823–832

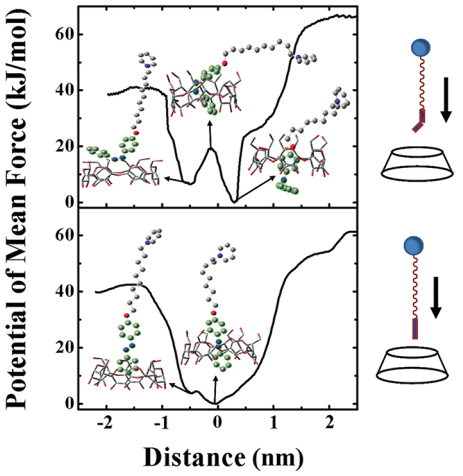

Figure 12. Potentials of mean force for AzoC10 to translocate through the cavity of α-CD, as a function of the center-of-mass distance between α-CD and the azobenzene moiety of AzoC10. The PMF for *cis*-AzoC10 is shown in the upper panel and that for *trans*-AzoC10 is shown in the lower panel. Each PMF represents Δ:↑ and ∇:↓ arrangements of the host and guest molecules. The typical structures observed along the reaction coordinate are displayed.

Potential of Mean Force Calculations. To further characterize the interactions between the host and guest molecules, the potentials of mean force for the guest molecules to pass through the cavity of α-CD from one side to the other were calculated with the umbrella sampling method. The center-of-mass distance between α-CD and the azobenzene moiety, projected along the central axis of the cavity of α-CD, was used to monitor the process of translocation, and it is constrained to certain reference values in the successive umbrella sampling simulations. The long alkyl chain of the guest molecule was free to move during the simulations. As described earlier, the guest molecule approached the host in four possible ways, Δ:↑, Δ:↓, ∇:↑, and ∇:↓, which led to two PMFs because Δ:↑ and ∇:↓ represent reversed processes and so do Δ:↓ and ∇:↑. The potential of mean force for *cis*-AzoC10 to translocate through the cavity from the side of primary rim to the side of secondary rim has been calculated and is shown in the upper panel of Figure 12, and that for *trans*-AzoC10 is shown in the lower panel. The PMFs shown in Figure 12 represent Δ:↑ and ∇:↓ arrangements of the host and guest molecules. The sign convention for the reaction coordinate is defined as follows. If the azobenzene moiety is on the side of the primary rim of α-CD, the reaction coordinate is negative. If the azobenzene moiety is on the side of the secondary rim of α-CD, the reaction coordinate is positive. The reaction coordinate is zero when the center-of-mass of the azobenzene moiety overlaps with that of α-CD in the direction of the central axis of α-CD.

For *trans*-AzoC10, an energy minimum was observed at the center-of-mass distance of about 0 nm. In the minimum, the azobenzene moiety of *trans*-AzoC10 is located at the cavity center of α-CD. The formation of the inclusion complexes is basically downhill in energy. These findings were consistent with those observed earlier in the MD simulations of assembly, indicating that the α-CD/*trans*-AzoC10 complexes have well-defined structures. Moving azobenzene out of the hydrophobic cavity of α-CD is associated with an energy cost of 45 kJ/mol. The shoulder in the PMF at the center-of-mass distance of −0.5 nm represents the configuration in which the azobenzene moiety is located right on top of the primary rim. It is noted that the calculated PMFs are not symmetric, the free energy of AzoC10 on one side of α-CD is higher than that on the other side, which indicates that the interactions between AzoC10 and α-CD are related to the orientations of the host and guest molecules.

In the case of *cis*-AzoC10, the PMF exhibits two minima. One minimum corresponds to the configuration in which the azobenzene moiety is located right above the primary rim of α-CD, before entering the cavity. The other minimum corresponds to the configuration in which one of the phenyl rings of azobenzene is exposed to the bulk water from the side of the secondary rim of α-CD. Between these two minima, there exists an energy barrier which corresponds to the configuration in which the bulky *cis*-azobenzene moiety is inside the cavity of α-CD. The barrier height is as high as 15 kJ/mol from one side of the PMF and 20 kJ/mol from the other side of the PMF, suggesting that the steric hindrance of *cis*-AzoC10 will prevent it from forming the inclusion complex with α-CD. Actually, we have shown in the earlier 10-ns simulations of the complexation that *cis*-AzoC10 can hardly assemble with α-CD. The shoulder observed at the center-of-mass distance of 0.5−1 nm corresponds to the configurations in which the long alkyl chain is included in the cavity of α-CD. The shuttling motion of α-CD over the hydrophobic tail of *cis*-AzoC10 has been observed in the 10 ns simulations. In the experiment of photocontrolled assembly and disassembly,[3] *trans*-AzoC10 formed the inclusion complex with α-CD. After UV irradiation, the *trans*-azobenzene moiety was transformed to the cis form. According to the PMF discussed above, it is anticipated that α-CD does not completely exclude the azobenzene moiety; instead one phenyl ring of *cis*-azobenzene is exposed to water. Therefore, the resulting α-CD/*cis*-AzoC10 complex is amphiphilic, which has explained why in the experiment the vesicle-like aggregates were observed but the size and shape of the aggregates were different from those formed in pure AzoC10 solution. In another setting of the experiment, UV light was used to irradiate the solution of pure *trans*-AzoC10 and then α-CD was added. After this treatment, aggregates similar to those of pure *trans*- formed the inclusion complex with α-CD. Our PMF calculation shows that *cis*-AzoC10 has to cross a high energy barrier of 15 kJ/mol to form the inclusion complex with α-CD, which can explain the above experimental observation.

4. CONCLUSIONS

The host−guest interactions between AzoC10 and α-CD have been investigated by the molecular dynamics simulations to reveal the role of photoisomerization in the photocontrolled reversible assembly and disassembly. The hydrophobic interactions between the host and guest molecules and the release of high-enthalpy water molecules from the cavity of α-CD are the major driving forces for the host−guest complexation. Our results of simulation showed that both *cis*-AzoC10 and *trans*-AzoC10 formed with α-CD the inclusion complexes that are energetically favorable, but the binding modes for the two isomers are rather different. The *trans*-azobenzene moiety fits into the cavity of α-CD very well, and the inclusion complexes have well-defined structures with azobenzene located at the center of the cavity. The host−guest inclusion for *trans*-AzoC10 is basically downhill in energy. The α-CD/*cis*-AzoC10 inclusion complexes are favored in energy as well, in which one phenyl ring

of *cis*-azobenzene is exposed to water. The shuttling motion of α-CD over the long hydrophobic tail of *cis*-AzoC10 was observed in the simulations. The bulky *cis*-azobenzene does not fit into the cavity of α-CD; therefore an energy barrier has to be overcome for *cis*-AzoC10 to complex with α-CD, so the host−guest inclusion is kinetically unfavorable for the cis form. The findings and analysis based on the all-atom MD simulations presented in the current work are consistent with the experimental observations, and provide a molecular picture of the photocontrolled assembly and disassembly. The supramolecular complexes formed between *cis*-AzoC10 and α-CD, as building blocks have shown extended assembly, forming the vesicle-like aggregates in aqueous solution. To disclose how the molecular structure of these building blocks affects the size and shape of the aggregates, simulations on larger time and length scales are needed.

AUTHOR INFORMATION

Corresponding Author

*E-mail: dong913@mail.tsinghua.edu.cn.

ACKNOWLEDGMENT

This work is supported by the National Natural Science Foundation of China (20903060) and the Foundation for Innovative Research Groups of the National Natural Science Foundation of China (21121004).

REFERENCES

(1) Ostro, M. J.; Cullis, P. R. *Am. J. Hosp. Pharm.* **1989**, *46*, 1576–1587.
(2) Vriezema, D. M.; Aragones, M. C.; Elemans, J. A. A. W.; Cornelissen, J. J. L. M.; Rowan, A. E.; Nolte, R. J. M. *Chem. Rev.* **2005**, *105*, 1445–1489.
(3) Wang, Y.; Ma, N.; Wang, Z.; Zhang, X. *Angew. Chem., Int. Ed.* **2007**, *46*, 2823–2826.
(4) Liu, K.; Wang, C.; Li, Z.; Zhang, X. *Angew. Chem., Int. Ed.* **2011**, *50*, 4952–4956.
(5) Yan, Q. A.; Yuan, J. Y.; Cai, Z. N.; Xin, Y.; Kang, Y.; Yin, Y. W. *J. Am. Chem. Soc.* **2010**, *132*, 9268–9270.
(6) Zhang, X.; Wang, C. *Chem. Soc. Rev.* **2011**, *40*, 94–101.
(7) Bender, M. L.; Komiyama, H. *Cyclodextrin Chemistry*; Springer-Verlag: New York, 1978.
(8) Tabushi, I. *Acc. Chem. Res.* **1982**, *15*, 66–72.
(9) Kinoshit., T; Iinuma, F.; Tsuji, A. *Biochem. Biophys. Res. Commun.* **1973**, *51*, 666–671.
(10) Kinoshit., T; Iinuma, F.; Tsuji, A. *Chem. Pharm. Bull.* **1974**, *22*, 2735–2738.
(11) Hoshino, M.; Imamura, M.; Ikehara, K.; Hama, Y. *J. Phys. Chem.* **1981**, *85*, 1820–1823.
(12) Turro, N. J.; Okubot, T.; Weed, G. C. *Photochem. Photobiol.* **1982**, *35*, 325–329.
(13) Arad-Yellin, R.; Eaton, D. F. *J. Phys. Chem.* **1983**, *87*, 5051–5055.
(14) Itoh, M.; Fujiwara, Y. *Bull. Chem. Soc. Jpn.* **1984**, *57*, 2261–2265.
(15) Ueno, A.; Takahashi, K.; Osa, T. *J. Chem. Soc., Chem. Commun.* **1980**, 921–922.
(16) Yorozu, T.; Hoshino, M.; Imamura, M. *J. Phys. Chem.* **1982**, *86*, 4426–4429.
(17) Cox, G. S.; Turro, N. J.; Yang, N. C. C.; Chen, M. J. *J. Am. Chem. Soc.* **1984**, *106*, 422–424.
(18) Turro, N. J.; Bolt, J. D.; Kuroda, Y.; Tabushi, I. *Photochem. Photobiol.* **1982**, *35*, 69–72.
(19) Turro, N. J.; Cox, G. S.; Li, X. *Photochem. Photobiol.* **1983**, *37*, 149–153.
(20) Scypinski, S.; Love, L. J. C. *Anal. Chem.* **1984**, *56*, 331–336.
(21) Lipkowitz, K. B. *Chem. Rev.* **1998**, *98*, 1829–1874.
(22) Sellner, B.; Zifferer, G.; Kornherr, A.; Krois, D.; Brinker, U. H. *J. Phys. Chem. B* **2008**, *112*, 710–714.
(23) Caballero, J.; Zamora, C.; Aguayo, D.; Yañez, C.; González-Nilo, F. D. *J. Phys. Chem. B* **2008**, *112*, 10194–10201.
(24) Zhang, H.; Feng, W.; Li, C.; Tan, T. *J. Phys. Chem. B* **2010**, *114*, 4876–4883.
(25) Brocos, P.; Díaz-Vergara, N.; Banquy, X.; Pérez-Casas, S.; Costas, M.; Piñeiro, Á. *J. Phys. Chem. B* **2010**, *114*, 12455–12467.
(26) El-Barghouthi, M. I.; Jaime, C.; Al-Sakhen, N. A.; Issa, A. A.; Abdoh, A. A.; Al Omari, M. M.; Badwan, A. A.; Zughul, M. B. *J. Mol. Struct. (THEOCHEM)* **2008**, *853*, 45–52.
(27) Hartley, G. S. *Nature* **1937**, *140*, 281–281.
(28) Nepogodiev, S. A.; Stoddart, J. F. *Chem. Rev.* **1998**, *98*, 1959–1976.
(29) Harada, A. *Acc. Chem. Res.* **2001**, *34*, 456–464.
(30) Wenz, G.; Han, B.-H.; Müller, A. *Chem. Rev.* **2006**, *106*, 782–817.
(31) Murakami, H.; Kawabuchi, A.; Kotoo, K.; Kunitake, M.; Nakashima, N. *J. Am. Chem. Soc.* **1997**, *119*, 7605–7606.
(32) Qu, D.-H.; Wang, Q.-C.; Ren, J.; Tian, H. *Org. Lett.* **2004**, *6*, 2085–2088.
(33) Tomatsu, I.; Hashidzume, A.; Harada, A. *J. Am. Chem. Soc.* **2006**, *128*, 2226–2227.
(34) Banerjee, I. A.; Yu, L.; Matsui, H. *J. Am. Chem. Soc.* **2003**, *125*, 9542–9543.
(35) Gornas, P.; Neunert, G.; Baczynski, K.; Polewski, K. *Food Chem.* **2009**, *114*, 190–196.
(36) Jullian, C.; Miranda, S.; Zapata-Torres, G.; Mendizabal, F.; Olea-Azar, C. *Bioorg. Med. Chem.* **2007**, *15*, 3217–3224.
(37) Szejtli, J. *Chem. Rev.* **1998**, *98*, 1743–1754.
(38) Van de Spoel, D.; Lindahl, E.; Hess, B.; Buuren, A. R.; Apol, E.; Meulenhoff, P. J.; Tieleman, D. P.; Sijbers, A. L.; Feenstra, K. A.; Drunen, R. et al. Gromacs User Manual version 3.3, 2005.
(39) Van Der Spoel, D.; Lindahl, E.; Hess, B.; Groenhof, G.; Mark, A. E.; Berendsen, H. J. C. *J. Comput. Chem.* **2005**, *26*, 1701–1718.
(40) Kirschner, K. N.; Yongye, A. B.; Tschampel, S. M.; González-Outeiriño, J.; Daniels, C. R.; Foley, B. L.; Woods, R. J. *J. Comput. Chem.* **2008**, *29*, 622–655.
(41) Tessier, M. B.; DeMarco, M. L.; Yongye, A. B.; Woods, R. J. *Mol. Simul.* **2008**, *34*, 349–363.
(42) Wang, J.; Wolf, R. M.; Caldwell, J. W.; Kollman, P. A.; Case, D. A. *J. Comput. Chem.* **2004**, *25*, 1157–1174.
(43) Frisch, M. J.; Trucks, G. W.; Schlegel, H. B.; Scuseria, G. E.; Robb, M. A.; Cheeseman, J. R.; Scalmani, G.; Barone, V.; Mennucci, B.; Petersson, G. A. et al. *Gaussian 09, Revision A.02*, Gaussian, Inc., Wallingford, CT, 2009.
(44) Bayly, C. I.; Cieplak, P.; Cornell, W.; Kollman, P. A. *J. Phys. Chem.* **1993**, *97*, 10269–10280.
(45) Cornell, W. D.; Cieplak, P.; Bayly, C. I.; Kollman, P. A. *J. Am. Chem. Soc.* **1993**, *115*, 9620–9631.
(46) Jorgensen, W. L.; Chandrasekhar, J.; Madura, J. D.; Impey, R. W.; Klein, M. L. *J. Chem. Phys.* **1983**, *79*, 926–935.
(47) Berendsen, H. J. C.; Postma, J. P. M; van Gunsteren, W. F.; DiNola, A.; Haak, J. R. *J. Chem. Phys.* **1984**, *81*, 3684–3690.
(48) Darden, T.; York, D.; Pedersen, L. *J. Chem. Phys.* **1993**, *98*, 10089–10092.
(49) Essmann, U.; Perera, L.; Berkowitz, M. L.; Darden, T.; Lee, H.; Pedersen, L. G. *J. Chem. Phys.* **1995**, *103*, 8577–8593.
(50) Humphrey, W.; Dalke, A.; Schulten, K. *J. Mol. Graphics* **1996**, *14*, 33–38.
(51) Torrie, G. M.; Valleau, J. P. *J. Comput. Chem.* **1977**, *23*, 187–199.
(52) Kumar, S.; Rosenberg, J. M.; Bouzida, D.; Swendsen, R. H.; Kollman, P. A. *J. Comput. Chem.* **1992**, *13*, 1011–1021.
(53) Kumar, S.; Rosenberg, J. M.; Bouzida, D.; Swendsen, R. H.; Kollman, P. A. *J. Comput. Chem.* **1995**, *16*, 1339–1350.
(54) Roux, B. *Comput. Phys. Commun.* **1995**, *91*, 275–282.

(55) Wei-Guang Diau, E. *J. Phys. Chem. A* **2004**, *108*, 950–956.
(56) Tiago, M. L.; Ismail-Beigi, S.; Louie, S. G. *J. Chem. Phys.* **2005**, *122*, 094311.
(57) Talaty, E. R.; Fargo, J. C. *Chem. Commun.* **1967**, *2*, 65–66.
(58) Bortolus, P.; Monti, S. *J. Phys. Chem.* **1987**, *91*, 5046–5050.
(59) Takei, M.; Yui, H.; Hirose, Y.; Sawada, T. *J. Phys. Chem. A* **2001**, *105*, 11395–11399.
(60) Yui, H.; Takei, M.; Hirose, Y.; Sawada, T. *Rev. Sci. Instrum.* **2003**, *74*, 907–909.
(61) Hingerty, B.; Klar, B.; Hardgrove, G. L.; Betzel, C.; Saenger, W. *Biomol. Struct. Dyn.* **1984**, *2*, 249–260.
(62) Tamai, N.; Miyasaka, H. *Chem. Rev.* **2000**, *100*, 1875–1890.